

# Far infrared properties of the rare-earth scandate $\text{DyScO}_3$

L. Baldassarre, A. Perucchi

*Sincrotrone Trieste S.C.p.A., S.S. 14 km 163.5,  
in Area Science Park, 34012 Basovizza (Trieste), Italy*

S. Lupi

*CNR-IOM and Dipartimento di Fisica,  
Università di Roma Sapienza, P.le A.Moro 2, 00185 Rome, Italy*

P. Dore

*CNR-SPIN and Dipartimento di Fisica,  
Università di Roma 'Sapienza, P.le A.Moro 2, 00185 Rome, Italy*

## Abstract

We present reflectance measurements in the infrared region on a single crystal the rare earth scandate  $\text{DyScO}_3$ . Measurements performed between room temperature and 10 K allow to determine the frequency of the infrared-active phonons, never investigated experimentally, and to get information on their temperature dependence. A comparison with the phonon peak frequency resulting from *ab initio* computations is also provided. We finally report detailed data on the frequency dependence of the complex refractive index of  $\text{DyScO}_3$  in the terahertz region, which is important in the analysis of terahertz measurements on thin films deposited on  $\text{DyScO}_3$ .

PACS numbers:

## I. INTRODUCTION

DyScO<sub>3</sub>, together with other rare-earth scandates (*R*ScO<sub>3</sub>), has recently received considerable attention, since it is considered to be among the best substrates for the epitaxial growth of high-quality ABO<sub>3</sub> perovskite-type thin films<sup>1</sup>. On such thin films it is possible to induce ferroelectric and multiferroic properties tailoring their lattice constants by changing *R* in *R*ScO<sub>3</sub>. For example, SrTiO<sub>3</sub> exhibits strain-induced ferroelectricity if grown on a RScO<sub>3</sub> substrate<sup>2</sup>. Furthermore, scandates are considered to be some of the most promising candidates to substitute SiO<sub>2</sub> as gate dielectric in MOSFET, thanks to the high value of their static dielectric constant  $\epsilon_0$ <sup>2,3</sup>. SrTiO<sub>3</sub>/DyScO<sub>3</sub> heterostructures are also widely used for applications in the terahertz (THz) range<sup>4</sup>.

We remark that scandates are increasingly used as substrates for film growth and that the optical investigation of a film often allows basic studies which can be difficult when only small size single crystals are available. In particular, the large and flat surface of a film permits accurate optical measurements in the far-IR and THz regions, which have an important role in studying superconducting films<sup>5</sup>. When the radiation penetration depth is larger than the film thickness the optical response of the substrate affects the measured far-IR/THz spectrum, and the complex dielectric function  $\tilde{\epsilon}(\omega) = \epsilon_1(\omega) + i\epsilon_2(\omega)$  of the film material cannot be obtained through the Kramers-Kronig (KK) transformations. In this case more elaborate procedures<sup>6,7</sup> must be used to extract the  $\tilde{\epsilon}(\omega)$  of the film from the reflectance or transmittance data, which require the knowledge of the substrate complex refractive index  $\tilde{n}(\omega) = n(\omega) + ik(\omega)$ . While the far-infrared properties of common perovskites-like substrates as SrTiO<sub>3</sub> and LaAlO<sub>3</sub> are well known<sup>8-10</sup>, no far-IR data are available in the DyScO<sub>3</sub> case. For this system, theoretical calculations of the phonon modes have been reported<sup>3</sup>, which could be compared only with data from recent Raman investigations<sup>11,12</sup>.

Moreover, both infrared (IR) and Raman spectroscopy are of interest in investigating the structural properties of oxide materials with the perovskite structure, since the study of the optical phonons can provide direct information on even subtle structural distortions of the ideal perovskite structure.

We have performed reflectance measurements in the IR region on a DyScO<sub>3</sub> single crystal, at a number of temperatures in the 10-300 K range. The infrared-active phonons of DyScO<sub>3</sub> have been investigated for the first time, allowing a direct comparison with the results of the

*ab initio* calculations<sup>3</sup>. Moreover the frequency and temperature dependence of the complex refractive index  $\tilde{n}(\omega)$  in the far-IR/THz region has been obtained.

## II. EXPERIMENTAL DETAILS AND RESULTS

Reflectance measurements were performed at near-normal incidence on the 110 surface of a DyScO<sub>3</sub> (DSO) single crystal. The sample was glued with silver paint, to ensure thermal contact, on an optically black cone<sup>13</sup> mounted on the end of a Helitran cryostat's coldfinger. Such cone was aligned, with the use of three tilting screws, so to have the sample surface perpendicular to the incident radiation. By employing a home-built reflectivity unit, measurements were performed over a broad energy range ( $50 \div 12000 \text{ cm}^{-1}$ ) with a Michelson interferometer at a spectral resolution of  $2 \text{ cm}^{-1}$ .

To obtain the absolute value of the reflectivity  $R(\omega)$  we employed the overfilling technique<sup>13</sup>. A metallic film of Au is deposited *in situ* on the sample surface and used as reference. This allows not only to prevent thermal disalignment but also to take into account any effect of diffraction due to the sample size or diffusion if the sample surface is not *mirror-like*.

The optical reflectivity  $R(\omega)$  is plotted up to  $800 \text{ cm}^{-1}$  in Fig. 1 at various temperatures. Several phonon lines, which show a weak temperature dependence, can be observed in this spectral region. At higher frequencies  $R(\omega)$ , in agreement with the insulating properties of the DyScO<sub>3</sub> crystal, is nearly flat and constant at a value of about 0.1 up to the highest measured frequency (see Fig.2).

## III. ANALYSIS AND DISCUSSION

DyScO<sub>3</sub> has an orthorhombically-distorted perovskite structure with space group *Pnma* with a 20-atom primitive cell. Therefore, one expects, as in the isostructural LaMnO<sub>3</sub> manganite<sup>14-17</sup>, 60 phonons, among which 24 are Raman active (corresponding to the irreducible representations  $7A_g$ ,  $5B_{1g}$ ,  $7B_{2g}$ ,  $5B_{3g}$ ), 25 are infrared active ( $9B_{1u}$ ,  $7B_{2u}$ ,  $9B_{3u}$ ), 8 silent ( $8A_u$ ), and 3 acoustic ( $B_{1u}$ ,  $B_{2u}$ ,  $B_{3u}$ ). By measuring the reflectance on the 110 surface, we should detect all the  $B_{1u}$  modes<sup>11,14-16</sup> corresponding to the dipole moment oscillating along  $z$ , where the orthorhombic axis  $z$  is defined as  $z = [001]$  (see Ref.<sup>11</sup> for more

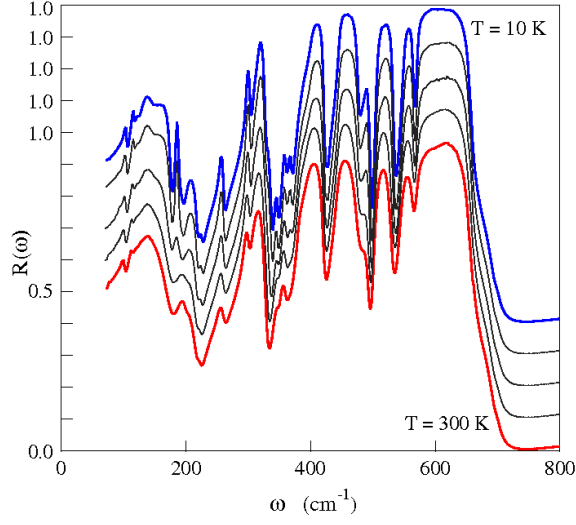


FIG. 1: (color online) Reflectivity of  $\text{DyScO}_3$  shown in the range of far-IR for  $T = 10\text{K}$ ,  $50\text{K}$ ,  $150\text{K}$ ,  $250\text{K}$  and  $300\text{K}$ . The curves are shifted of 0.1 along the vertical axis for sake of clarity.

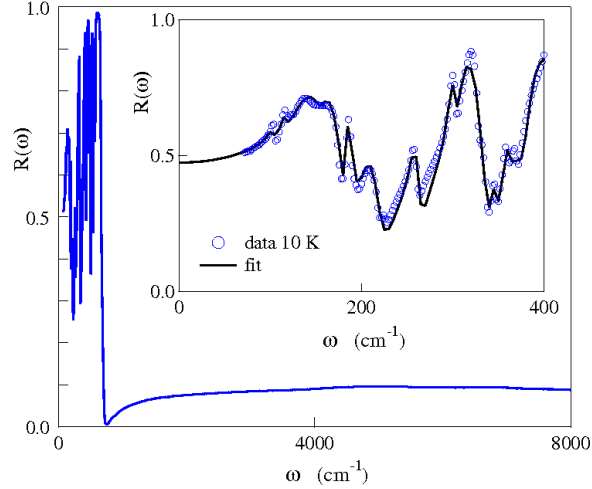


FIG. 2: (color online) Reflectivity of  $\text{DyScO}_3$  at  $T = 10\text{ K}$  shown up to  $8000\text{ cm}^{-1}$ . In the inset the low-frequency  $R(\omega)$  is compared with a fit obtained from the Lorentz model.

details), and a linear combination of the  $B_{2u}$  and  $B_{3u}$  corresponding to the dipole oscillating along  $y$  and  $x$ , respectively<sup>15</sup>.

In order to perform the KK analysis<sup>6</sup>, we first performed a Lorentz fit on  $R(\omega)$  so to extrapolate its behavior as  $\omega \rightarrow 0$ . We have fitted the low-frequency part of  $R(\omega)$  (*i.e.* below  $400\text{ cm}^{-1}$ ) in order to obtain a careful description in the THz region. This procedure

resulted in a convincing extrapolation of the experimental data down to zero frequency and in reliable results in the far-IR once the KK transformations are performed. We remark that data have been collected up to  $12000\text{ cm}^{-1}$ , so to avoid problems in the KK procedure due to the high-frequency extrapolation of the spectra. The resulting  $\epsilon_2(\omega)$  are reported in Fig. 2 for frequencies below  $600\text{ cm}^{-1}$  at selected temperatures.

At 10 K, 19 of the expected 25 IR-active modes are clearly visible in the spectrum. As in the case of the isostructural  $\text{LaMnO}_3$  system, the three phonon modes (external, bending, and stretching modes) proper of the cubic perovskite structure<sup>18</sup> are split in several phonons because of the orthorhombic distortion. The low frequency phonon modes originate from the external mode, i.e. are due to vibrations of the Dy-cation sublattice with respect to the network of  $\text{ScO}_6$  octahedra. The high frequency phonons originate from the stretching mode of oxygens in the  $\text{ScO}_6$  octahedra, the phonons at intermediate frequencies from the bending mode. However, due to the strong orthorhombic lattice distortions, none of the modes can be classified as purely bending or as purely stretching as these modes imply considerable changes of both the bond angles and bond lengths in the  $\text{ScO}_6$  octahedra<sup>15</sup>. In the vibrational spectra we distinguish one phonon mode around  $100\text{ cm}^{-1}$  and one around  $115\text{ cm}^{-1}$ . These frequencies are close to those predicted by *ab initio* calculations for a  $B_{3u}$  and a  $B_{1u}$  modes, respectively. Their dipole moment is due to small displacements of Sc-O ions *vs* Dy that do not compensate along the  $x$  direction<sup>3</sup> while the larger vertical ( $z$ ) displacements produce no dipole moment. The intensity of these modes can in principle be enhanced by disorder, which can also increase the static dielectric constant  $\epsilon_0$ .

To determine the central frequency of the phonon modes and their temperature dependence, we have fitted  $\epsilon_2(\omega)$  within the Lorentz model by using:

$$\tilde{\epsilon} = \epsilon_1(\omega) + i\epsilon_2(\omega) = \epsilon_\infty + \sum_j \frac{A_j \omega_j^2}{\omega_j^2 - \omega^2 - i\omega\gamma_j} \quad (1)$$

where  $A_j$ ,  $\omega_j$  and  $\gamma_j$  are respectively the mode strength, the central frequency and the damping of each phonon mode  $j$ . The resulting curves obtained with  $\epsilon_\infty \sim 4$  are in good agreement with the data, as shown for  $T = 10\text{ K}$  and  $300\text{ K}$  in Fig.3. The phonon frequencies resulting from the fits are reported in Table I and tentatively compared with the calculations of Ref.<sup>3</sup> As our measurements were performed without polarizing the incoming beam no information about the polarization of the phonon peaks can be extracted from the experimental data. We made a tentative assignment by simply comparing the phonon frequencies

obtained from the fit with the computed ones. Taking into account the complexity of this class of materials, we believe that the overall agreement between theory and experiment should be considered as reasonable.

Most of the phonons harden their central frequency with decreasing  $T$  and reduce their half-height half-width  $\gamma$ , as expected and in good agreement with the behavior found in Ref.<sup>12</sup> at higher temperatures. A closer inspection of data shows that the broad peak, visible at 300 K just below  $200\text{ cm}^{-1}$  is due to two different phonon modes at  $190\text{ cm}^{-1}$  and at  $199\text{ cm}^{-1}$  (see Table I). The apparent splitting of such peak is due to the softening of the more intense mode (at  $190\text{ cm}^{-1}$ ) to  $185\text{ cm}^{-1}$  and the simultaneous hardening of the second mode. Some other weak modes also show a light softening by decreasing  $T$  as reported in Table.I. This softening might correspond to subtle lattice modifications (still within the  $Pnma$  crystal structure) as  $T$  decreases. To the best of our knowledge, the  $T$ -behavior of the  $\text{DyScO}_3$  lattice parameters has been investigated between 298 - 1273 K, that is the temperature range of interest for perovskite thin film growth<sup>19</sup>, while no data exist at lower temperatures. Therefore one cannot link unambiguously the modifications in the IR-active phonon response to a structural rearrangement.

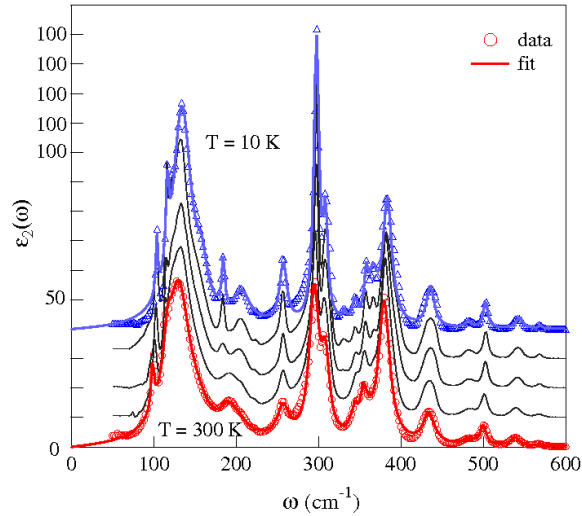


FIG. 3: (color online): Imaginary part  $\epsilon_2(\omega)$  of the complex dielectric function of  $\text{DyScO}_3$ . Data are shown at a number of temperatures and shifted for sake of clarity. At 10 K and 300 K both data and Lorentz fitting are reported.

TABLE I: Experimental phonon frequencies obtained by means of IR measurements (at 300 K and 10 K) compared with theoretical calculations, from Ref.<sup>3</sup>

$\omega_{exp}$ (cm <sup>-1</sup> )	$\omega_{exp}$ (cm <sup>-1</sup> )	$A_j$ 10 K	$\omega_{theo}$ (cm <sup>-1</sup> )	Mode Symmetry
300 K	10 K	10 K	Ref.3	Ref.3
101	104	0.52	97.9	B <sub>3u</sub>
113	117	0.96	111.0	B <sub>1u</sub>
131	135	15.35	129.4	B <sub>2u</sub>
160	159	1.12	173.7	B <sub>1u</sub>
190	185	0.37	193.3	B <sub>2u</sub>
199	205	1.14	197.0	B <sub>3u</sub>
-	-	-	231.4	B <sub>3u</sub>
256	257	0.85	278.8	B <sub>1u</sub>
-	-	-	283.2	B <sub>2u</sub>
-	-	-	285.3	B <sub>3u</sub>
295	298	2.53	293.9	B <sub>1u</sub>
306	309	0.69	328.8	B <sub>1u</sub>
344	332	0.04	334.4	B <sub>3u</sub>
346	344	0.14	336.4	B <sub>2u</sub>
354	358	0.23	356.7	B <sub>3u</sub>
371	367	0.44	368.6	B <sub>2u</sub>
381	385	1.51	369.5	B <sub>1u</sub>
-	-	-	412.9	B <sub>1u</sub>
-	-	-	419.2	B <sub>3u</sub>
434	436	0.35	435.5	B <sub>2u</sub>
-	-	-	445.3	B <sub>2u</sub>
-	-	-	478.1	B <sub>3u</sub>
484	482	0.03	484.8	B <sub>1u</sub>
501	503	0.12	509.7	B <sub>1u</sub>
539	544	0.07	532.6	B <sub>3u</sub>
570	570	0.07	-	

It is important to notice that the low-frequency modes, due to vibrations of the  $R$ -cation sublattice with respect to the  $\text{ScO}_6$  octahedral network, are those with higher intensity. This finding supports the theoretical prediction<sup>3</sup> that in  $\text{DyScO}_3$  the high value of the static dielectric constant  $\epsilon_0$ , i.e.  $\tilde{\epsilon}(\omega \rightarrow 0)$ , is associated with low-frequency ionic vibrations. On the basis of the employed procedure,  $\epsilon_0$  is given by  $\epsilon_\infty + \sum_j A_j$  (see Eq.1). Since the fitting procedure provides the  $A_j$  value for each mode (as reported in Table I), we find that the phononic contribution to  $\epsilon_0$ , i.e.  $\sum_j A_j$  is large, of about 21, mainly due to the phonon mode at  $135 \text{ cm}^{-1}$ . Moreover we find a total static dielectric constant  $\epsilon_0 \approx 25$ , as the sum of  $\epsilon_\infty \sim 4$  and the phononic contribution, in excellent agreement with theory<sup>3</sup> and experiments on single crystals<sup>2</sup>.

Finally we report in Fig.4 the frequency dependance of the complex refractive index  $\tilde{n} = n + ik$  in the THz region as directly obtained from  $\tilde{\epsilon} = \epsilon_1 + i\epsilon_2$ . Below  $100 \text{ cm}^{-1}$   $n$  is nearly flat reaching a value of about 5 for  $\omega \rightarrow 0$ , while the vanishingly small  $k$  value indicates the absence of an appreciable absorption in the same spectral region.

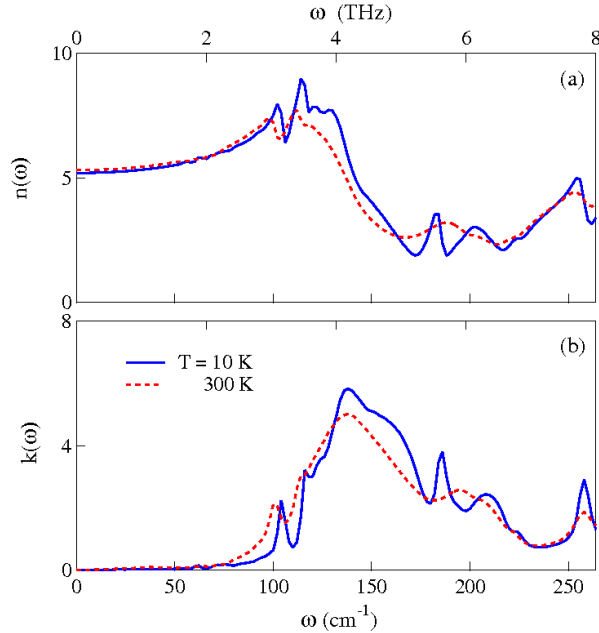


FIG. 4: (color online): a) Real and b) Imaginary part of  $\tilde{n}$  for  $\text{DyScO}_3$  at 10 and 300 K in the THz range.

The  $n$  and  $k$  data at 10 K have been recently employed in the analysis of the THz

measurements performed on a film<sup>20</sup>, grown on a DSO substrate<sup>21</sup>, of the  $\text{BaFe}_{1.84}\text{Co}_{0.16}\text{As}_2$  compound, that belongs to the class of the new Fe-based superconductors which attracted strong attention since their recent discovery<sup>22</sup>.

#### IV. CONCLUSIONS

We have presented here the first experimental data on the IR phonon spectrum of the rare earth scandate  $\text{DyScO}_3$ . In the temperature range between 10 and 300 K no dramatic changes occur in the phonon response indicating that the  $Pnma$  structure is stable down to the lowest measured temperature. The overall agreement with the recent *ab initio* calculations is to be considered satisfactory. We finally note that the present work can provide reference data and extrinsic peak selection for future infrared investigations of thin films grown on  $\text{DyScO}_3$  substrates.

- 
- <sup>1</sup> Uecker, R., Velickov, B., Klimm, D., Bertram, R., Bernhagen, M., Rabe, M., Albrecht, M., Fornari R., and Schlom, D.G., *Journal of Crystal Growth*, **310**, 2649 (2008).
  - <sup>2</sup> Haeni, J.H., Irvin, P., Chang, W., Uecker, R., Reiche, P., Li, Y.L., Choudhury, S., Tian, W., Hawley, M E., Craigo,B., Tagantsev, A.K., Pan, X.Q., Streiffer, S.K., Chen, L.Q., Kirchoefer, S.W., Levy, J., and Schlom, D.G., *Nature*, **430**, 758, (2004).
  - <sup>3</sup> Delugas, P., Fiorentini, V., Filippetti, A., and Pourtois, G., *Phys. Rev. B*, **75**, 115126 (2007).
  - <sup>4</sup> Kuzel, P., Kadlec, F. Petzelt, J., Shubert, J., Panaitov, G., *Appl. Phys. Lett.*, **91**, 232911 (2007).
  - <sup>5</sup> Tinkham, M., *Introduction to Superconductivity*, McGraw-Hill, New York (1975)
  - <sup>6</sup> Dressel, M., and Grüner, G., *Electrodynamics of Solids*, Cambridge University Press, Cambridge, England (2002).
  - <sup>7</sup> Berberich, P., Chiusuri, M., Cunsolo, S., Dore, P., Kinder, H., Varsamis, C.P., *Infrared Phys.* **34**, 269 (1993).
  - <sup>8</sup> Calvani, P., Capizzi, M., Donato, F., Dore, P., Lupi, S., Maselli, P., Varsamis, C.P. *Physica C* **181**, 289 (1991).
  - <sup>9</sup> Zhang, Z.M., Choi, B.I., Flik, M.I., and Anderson, A.C., *J. Opt. Soc. Am. B* **11**, 2252 (1994)
  - <sup>10</sup> Dore, P., Paolone, A., and Trippetti, R., *J. Appl. Phys.* **80** 5270 (1996); Dore, P., De Marzi, G.,

- and Paolone, A., *Int. J. of IR and mm Waves*, **18**, 125 (1997).
- <sup>11</sup> Chaix-Pluchery, O., and Kreisel, J., *J. Phys.: Condens. Matter* **21**, 175901 (2009).
  - <sup>12</sup> Chaix-Pluchery, O., and Kreisel, J., *J. Phys.: Condens. Matter* **22** 165901 (2010).
  - <sup>13</sup> Homes, C.C., Reedik, M., Cradles, D.A., and Timusk, T., *Appl. Optics* **32**, 2976 (1993).
  - <sup>14</sup> Iliev, M.N., Abrashev, M.V., Lee, H.-G., Popov, V.N., Sun, Y.Y. Thomsen, C., Meng, R.L. and Chu, C.W., *Phys. Rev. B* **57**, 2872 (1998).
  - <sup>15</sup> Fedorov, I., Lorenzana, J., Dore, P., De Marzi, G., Maselli, P., Calvani, P., Cheong, S-W., Koval, S., and Migoni, R., *Phys. Rev. B* **60**, 11875 (1999).
  - <sup>16</sup> Smirnova, I.S., *Physica B* **262**, 247 (1999).
  - <sup>17</sup> Paolone, A., Roy, P., Pimenov, A., Loidl, A., Melnikov, O.K., and Shapiro, A.Ya., *Phys. Rev. B* **61**, 11255 (2000).
  - <sup>18</sup> Burns, G., *Solid State Physics* Academic Press, Boston, 1990.
  - <sup>19</sup> Biegalski, M.D., Haeni, J.H., Trolier-McKinstry, S., Schlom, D.G., Brandle, C.D., and Ven Graitis, A.J., *J. Mater. Res.*, **20**, 952 (2005).
  - <sup>20</sup> Perucchi, A., Baldassarre, L., Marini, C., Lupi, S., Jiang, J., Weiss, J.D., Hellstrom, E.E., Lee, S., Bark, C.W., Eom, C.B., Putti, M., Pallecchi, I., and Dore, P., *EPJ B*, *in press* (2010).
  - <sup>21</sup> Lee, S., Jiang, J., Zhang, Y., Bark, C.W., Weiss, J.D., Tarantini, C., Nelson, C.T., Jang, H.W., Folkman, C.M., Baek, S.H., Polyanskii, A., Abraimov, D., Yamamoto, A., Park, J.W., Pan, X.Q., Hellstrom, E.E., Larbalestier, D.C., and Eom, C.B., *Nat. Mat.*, **9**, 397, (2010).
  - <sup>22</sup> Kamihara, Y., Watanabe, T., Hirano, M., and Hosono, H., *J. Am. Chem. Soc.* **130**, 3296 (2008).